Int. J. Nano Dimens., 9 (1): 79-88, Winter 2018

ORIGINAL ARTICLE

Comparison of different kinetic models for adsorption of acid blue 62 as an environmental pollutant from aqueous solution onto mesoporous Silicate SBA-15 modified by Tannic acid

Alireza Golshan Tafti[1]; Abosaeed Rashidi[1,]; Habib-Allah Tayebi[2]; Mohammad Esmaeil Yazdanshenas[3]*

[1]*Department of Textile Engineering, Science and Research Branch, Islamic Azad University, Tehran, Iran*
[2]*Department of Textile Engineering, Qaemshahr Branch, Islamic Azad University, Qaemshahr, Iran*
[3]*Department of Textile Engineering, Yazd Branch, Islamic Azad University, Yazd, Iran*

Received 08 June 2017; revised 20 September 2017; accepted 03 December 2017; available online 05 December 2017

Abstract

In this work, adsorption kinetics were investigated in order to remove the acid blue 62 off the aqueous solutions using mesoporous silicate SBA-15 loaded with tannic acid (tannin-SBA-15). Nitrogen adsorption and desorption test (BET), X-ray diffraction (XRD) and Fourier transform infra-red spectroscopy (FT-IR) analysis characterize synthesized composite. The impacts of some parameters such as PH, adsorbent dosage as well as contact time were studied and optimized at temperatures between 25 to 45 °C. The study also was conducted on intra-particle diffusion, pseudo first-order, pseudo second-order and Elovich kinetic models. In order to have the best correlation with the experimental data, the model of the second-order kinetics was discovered. The model of the intra-particle diffusion represents that both boundary layer and intra-particle diffusion processes control the mechanisms of adsorption of acid blue 62 onto tannin-SBA-15.

Keywords: *Acid blue 62; Adsorption; Adsorption kinetic model; SBA-15; Tannic acid.*

How to cite this article

Golshan Tafti A R, Rashidi A, Tayebi H, Yazdanshenas M E. Comparison of different kinetic models for adsorption of acid blue 62 as an environmental pollutant from aqueous solution onto mesoporous silicate SBA-15 modified by tannic acid. Int. J. Nano Dimens., 2018; 9 (1): 79-88.

INTRODUCTION

Nowadays, in order to remove dyes and pollutants from industrial effluents a number of techniques are applied. One of the useful and applicable physicochemical techniques is adsorption. High adsorption capacity of adsorbents and fast kinetics are significant factors for adsorption systems. Different types of dyes are utilized by such industries as dyestuffs textile, paper, plastics, and pharmaceuticals [1]. Most of the dyes which are released into the environment are poisonous and carcinogenic. In order to eliminate the pollutants from aqueous solutions, it is appropriate to use low-cost matters such as agricultural wastes containing high amounts of polyphenols. Researchers have studied the adsorption properties of natural plants like waste sugar beet pulp [2], degreased coffee bean [3], garlic peel [4], pumpkin seed hull [5], olive pomace [6], orange peel activated carbon [7], potato plant wastes [8] and cotton plant wastes [9]. To adsorb the contaminants from aquatic environments, tannic acid as a natural plant which contains high amounts of multiple phenolic hydroxyls is a suitable and efficient adsorbent. Water solubility existing in tannic acid limits its application as the adsorbent in the aqueous solutions, so jellification and immobilization of tannin onto water-insoluble materials like agarose, cellulose, silicates and collagen fiber improve its performance for adsorption process [10]. Despite the proper capacity of tannin, few researches have focused on the usage of tannin as an efficient adsorbent.

Rosa Canina Galls was investigated by Bagd et al. [11].They studied the Basic Blue 9 and Basic Violet 3 adsorption on low-cost adsorbents. The adsorption features of modified quebracho tannin resin (QTR) were investigated by Meral Yurtsever

* Corresponding Author Email: *rashidi50@yahoo.com*

et al. in order to remove Pb (II) ions [12]. They concluded that QTR is a practical adsorbent with high adsorption capacity of Pb (II) ions. Mesoporous materials with large meso pores volume which possess high surface area and the pore size distribution have been considered as efficient and appropriate insoluble supports. The adsorption capacity of mesoporous is affected by surface modification of the mesoporous materials and could be obtained by grafting or in-situ synthesis techniques. Also, mesoporous materials with large specific surface area cause uniform distribution of functional groups.

Surface modified mesoporous materials as the effective adsorbents have been introduced in different studies in order to remove the contaminants. The adsorption characteristics of polypyrrole modified SBA-15 nanocomposite for eliminating of Hg (II) from aqueous media [13] were investigated by Shafiabadi *et al.* Qiang Gao et al. synthesized composites of natural polymer chitosan (CTS) and siliceous mesoporous SBA-15, i.e. SBA-15/CTS (5%), SBA-15/CTS (10%), and SBA- 15/CTS (20%), by prehydrolysis of tetraethyl orthosilicate in the presence of pore-directing agent and subsequent condensation with an appropriate amount of CTS-based organosilane [14]. The adsorption performance of the prepared composites to eliminate acid red 18 (AR18) was studied. Aminopropyl and β-cyclodextrin functionalized HMS (HMS-NH_2 and HMS-CD) were synthesized by Asouhidou *et al.* [15] and applied to remove Remazol Red 3BS. Both HMS-NH_2 and HMS proved to have lower adsorption capacity than that of HMS-CD adsorbent. The adsorption of acid dye (acid blue 62) was studied by Torabinejad *et al.* on ammonium modified MCM-41 (NH_3^+-MCM-41) [16].

As mentioned previously, to inhibit the solubility of tannin in aqueous media, it should be immobilized on the surface of the materials which are soluble in water such as mesoporous silicates. Xin Huang and co-workers synthesized tannin-functionalized mesoporous silica (BT–SiO_2) and this adsorbent was studied for its adsorption capacity for removing chromium cations from aqueous media [17]. Lower specific surface area of tannin inhibits the activity and application of tannin as a useful adsorbent. Therefore, it takes a long time to achieve equilibrium state and increases equilibrium time. So, the uniform distribution of tannin existing on the surface of mesoporous silicate which enjoys high surface area, prepares the suitable adsorbents for association in the adsorption process. Up to now, no instances have been reported about synthesizing of tannin modified mesoporous SBA-15. The aim of this study is to prepare tannic acid-SBA-15 mesoporous nanocomposite and evaluation of its capacity to remove acid blue 62. Moreover, after investigating the kinetics of the adsorption process, mechanism of adsorption was determined.

EXPERIMENTALS

Materials

Tetraethyl ortho silicate (TEOS, $SiC_8H_{20}O_4$), Pluronic P123 surfactant ($EO_{20}PO_{70}EO_{20}$, Mw=5800), Na_2HPO_4 and NaH_2PO_4 for buffer solution, tannic acid as source of polyphenol, 3-Aminopropyltriethoxysilane), glutaraldehyde (50%, w/w), hexane, HCl and NaOH for pH adjustment and deionized water were purchased from Merck. Moreover, acid blue 62 (λ_{max}=665 nm, Fig. 1) was purchased from Dystar, Germany.

Synthesis of mesoporous SBA-15

Zhao et al. proposed a protocol that on its basis mesoporous SBA-15 was prepared as following [18]: 90 mL of deionized water is enough to dissolve 2 g of P123 as surfactant. After being stirred for 4h and also the observation of transparent solution, 180 mL of HCl (2M) was added with 2 h stirring at 40 °C. Then, 26.4 g of TEOS as the silica source was poured, the consequent gel was stirred at 40 °C for 24 h with heating up to 100 °C in a period of 48 h. Filtering was conducted on the solid product, after that they were washed for more times with water/ethanol, and then they were dried in a period of 24 h at 100 °C. To remove the template P123 and existing organics inside the as-synthesized

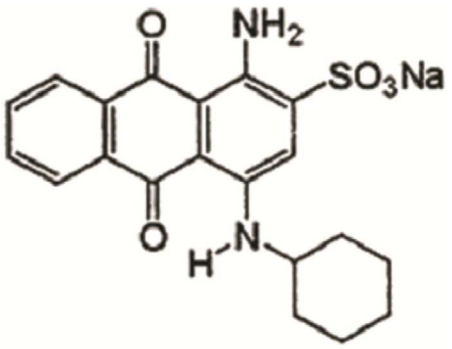

Fig. 1: Chemical structure of acid blue 62.

mesoporous, the obtained product was put in the furnace at 550 °C for 5 h.

Preparation of aminated SBA-15

In order to prepare aminated SBA-15 nano-powders, 2.00g of SBA-15 and 10mL of 3-aminopropyltriethoxysilane (APTES) were added in 250 mL round-bottom flask which contains 50 mL of normal hexane. Then, under the reflux and for a period of 6 h, the mixture was stirred. After that, filtering, washing with acetone and deionized water, and eventually drying for 24 h in vacuum condition at 323K were done on the prepared product.

Tannic acid–SBA-15 nanocomposie synthesis

Phenolic rings of tannic acid are nucleophile; so, covalent bonds with these rings can be made by some electrophilic agents such as glutaraldehyde. Since the immobilization of tannic acid on the surface of SBA-15 is favorable, glutaraldehyde which is considered a cross-linking agent can react with the amino group of aminated SBA-15 and forms the covalent bond [19]. For preparation of tannic acid/SBA-15 nanocomposite, aminated SBA-15(2 g) was mixed with 1% tannic acid solution. Then, stirring took place for 2h on the mixture at room temperature. After that, 6 mL of glutaraldehyde (50%, w/w) was added to the mixture. Then, 24 hours of stirring was done on the mixture at 298 K. Subsequently, after the filtration, the acts of washing with deionized water and drying in the oven at 323K were performed on the mixture until the brown tannic acid – SBA -15 nanocomposite was obtained.

Tannin immobilization on the surface of aminated SBA-15 was calculated according to the difference of tannic acid solution concentration and ultraviolet-visible spectrophotometer was used for its measurement (6310, JENWAY, UK) [1, 19]. The loading of 1% tannin solution on aminated SBA-15 was approximated about 36%. Fig. 2 depicts the route of the tannin-aminated SBA-15 nanocomposite synthesis.

Instrumentation

The analysis of the X-ray diffraction (XRD) which confirms the crystalinity of synthesized SBA-15 was engaged in the scope of 2θ=0-10° utilizing reflactometer (XRD, Philips instruments, Australia, 35kV, 28.5mA, 25 °C and copper anode as a radioactive source). For determination of the concentrations of dye solutions, UV-visible spectrophotometer was used before and also after the adsorption. To calculate the surface area of the BET prepared samples, the linear part of BET plot was applied. Also, the distribution of the Ppre size and Pore volume distribution were determined using BJH (Barret-Joyner-Halenda) method which is from the adsorption curve of N_2 of the adsorption-desorption isotherm (Quantachrome NovaWin2, USA). Fourier transform infrared spectrometry (FTIR, 8400S, Shimadzu, Japan, KBr technique) technique with the wave numbers range of 400–4000 cm^{-1} was applied to confirm the coverage of SBA-15 surface by amine and tannin.

Adsorption procedure

Shaker incubator was used to perform Batch experiments with the control of the speed of shaking containing 100 mL of dye solutions by first dye concentrations of 40 up to 600 mg L^{-1}. Each Erlenmeyer contains optimal dosage of tannic acid-SBA-15 nanopowder at the optimum pH. The impacts of some significant parameters such as temperature, the contact time, pH and adsorbent dosage were examined. Samplings were done for each concentration and after 5, 15, 30, 45, 60, 90 and 120 minutes of contact times. Then, each sample was centrifuged at 5000 rpm for 30 minutes. Ultraviolet-visible spectrophotometer was used to measure the dye absorbance in maximum wavelength (λ_{max}=665 nm) in order to estimate the equilibrium concentration. Following formula [15] is applied to measure the adsorption capacity:

$$q_t = (C_i - C_t) \times V/M \quad (1)$$

Where q_t (mg/g) is considered as the adsorption capacity, C_i and C_t (mg/L) are known as the dye concentrations at beginning time and any time *t*, *V* and *M* are the volumes of dye solution (L) and the mass of adsorbent (g), respectively.

The removal efficiency was calculated by below formula:

$$\text{Removal efficiency (\%)} = (C_i - C_t)/C_i \times 100 \quad (2)$$

RESULTS AND DISCUSSION

Characterization analysis

The FTIR spectra of SBA-15, Aminated-SBA-15 and Tannin-aminated SBA-15 were prepared in the scope of 400–4000 cm^{-1}. The existence of tannin and amine on the SBA-15 can be proved by FTIR analysis. In Fig. 3, a wide band in the scope of 3000-3700 cm^{-1} represents the presence of Si-

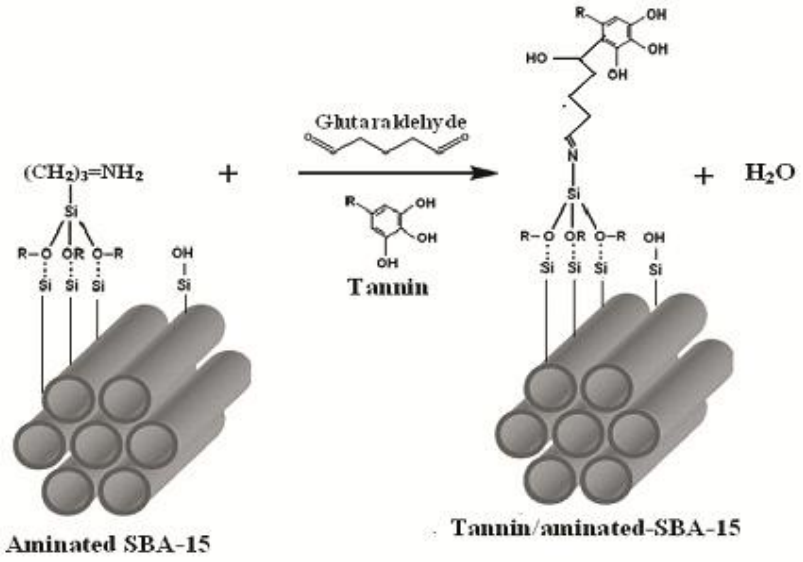

Fig. 2: Synthesis route for tannic acid-SBA-15 adsorbent.

OH groups. The sharp peak at 1087 cm^{-1} shows asymmetric stretch of vibrations of Si-O band in Si-O-Si and peaks at 465 cm^{-1} and 802 cm^{-1} are related to the both bending and symmetric stretch vibrations of Si-O-Si, respectively [13,14]. The stretch vibration of – OH (phenolic and alcoholic groups) in tannin structure like – OH in the hydrogen-bonded of water (Tannin-aminated SBA-15) can be seen in the scope of 3000–3700 cm^{-1} and reach the peak at 3443 cm^{-1}. The peak at 2925 cm^{-1} can be ascribed to the stretch vibrations of aromatic C–H and methylene (– CH_2 –) [20, 21]. The absorption band at 2363 cm^{-1} is due to the presence of carboxyl group compound [22]. Moreover, the peaks in the range of 1450–1650 cm^{-1} demonstrate aromatic rings [23]. The peak at 1088 cm^{-1} confirms the stretching vibrations of C–O–C [24]. The descent of peak intensities in the scope of 3000-3700 cm^{-1} and at 1087 cm^{-1} shows the formation of SBA-15 nano-powders.

The patterns of low angle XRD of synthesized SBA-15 and Tannin-aminated SBA-15 in the range of $0 < 2\theta < 10$ containing three peaks are shown in the Fig. 4. The strong and sharp peak (10 0) at $0 < 2\theta < 1$ and two weak peaks (110) and (2 0 0) at $1 < 2\theta < 2$ indicate the hexagonal structure of silicate mesopore SBA-15 [13, 14]. As can be seen, loading of SBA-15 by tannic acid has no effect on the XRD pattern while reduction of peak intensity is observed for tannin-aminated SBA-15. This reduction is attributed to filled channels of SBA-15 by tannic acid and amine [16, 17]. According to this result, applying nanocomposites for the adsorption of the dye has created no change in its crystal structures, but due to the filling of the porosity of adsorbent, has decreased its severity. Furthermore, the decline of the surface area of BET, the pore size and the

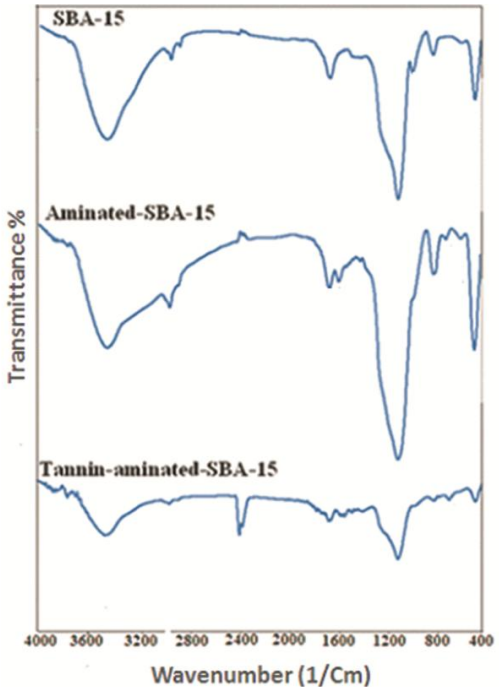

Fig. 3: FT-IR spectra of the SBA-15, Aminated-SBA-15 and Tannic acid-aminated ABA-15.

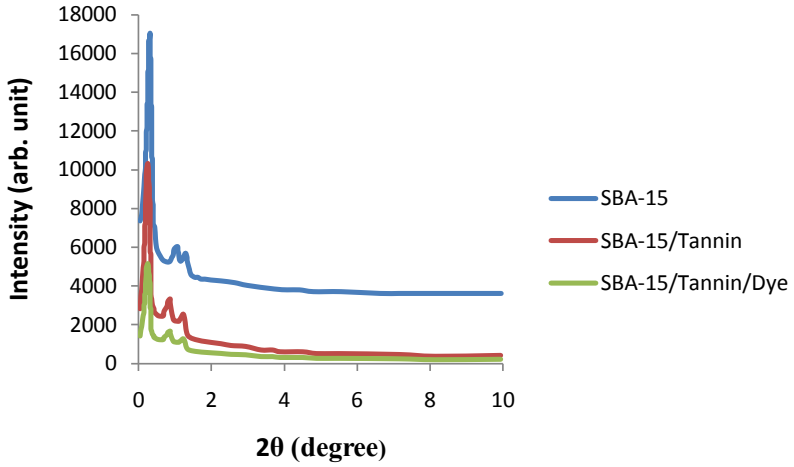

Fig. 4: XRD patterns of the SBA-15 and SBA-15/Tannin.

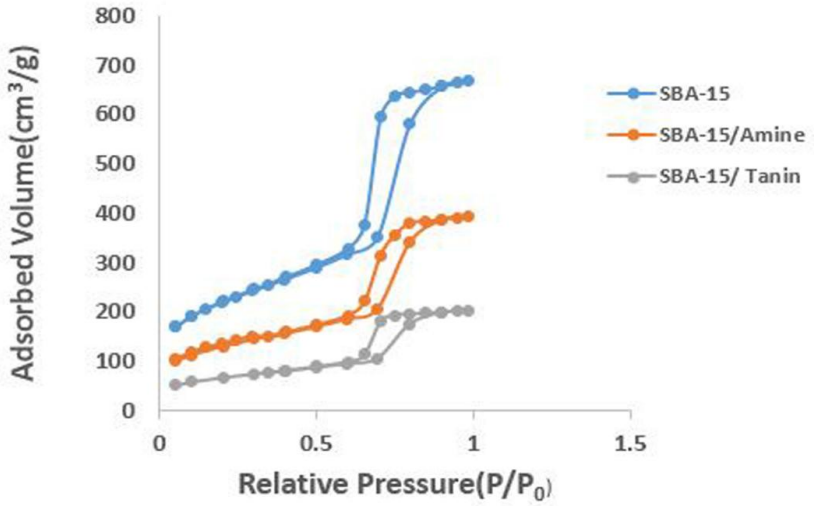

Fig. 5: The effect of pH on dye removal percentage and adsorption capacity of SBA-15 and tannic acid-SBA-15.

volume of Tannin-aminated SBA-15 nano-composite obviously shows well coverage of SBA-15 channels by amine and tannin [13,16,17]. SBA-15 pore size was assessed about 8.2 nm (BJH method) which is not as large as the d spacing 9.3 nm for plane (10 0) of XRD pattern.

The N_2 adsorption and desorption isotherms of the SBA-15 and Tannin-aminated SBA-15 nano-composites are shown in Fig. 5. As can be seen, isotherm of type IV containing loop (hysteresis) is sizable for SBA-15. A sharp increase of adsorbed N_2 which is the specification of mesoporous materials is shown at P/P_0 = 0.6–0.8 [15, 24-25]. Also, results of the BJH method show narrow PSD and average pore size of 8.2 nm for SBA-15. Specifications of SBA-15 and nanocomposites are presented in Table 1. The reduction of BET, volume and pore size of aminated SBA-15 and Tannin-aminated SBA-15 clearly shows the penetration of amine and tannin into the channels of SBA-15. According to the Table 1, the BET surface area of SBA-15 reduced from 714.5 m^2/g to 390.7 and 199.2 m^2/g after loading by amine and tannic acid, respectively. This loading obstructs the pores and causes the decrease of the BET surface area. The BET curve of adsorption data and BJH analysis were utilized to estimate the special surface area and PSD of the synthesized adsorbent and the outcomes are tabulated in Table 1.

Table 1: Texture parameters of SBA-15, Aminated-SBA-15 and Tannin-aminated ABA-15.

Sample	Surface area (BET)[a] (m^2/g)	Pore diameter[b] (nm)	Pore Volume[c] (BJH) (cm^3/g)
SBA-15	714.5	8.2	0.98
Aminated SBA-15	390.7	5.2	0.68
Tannin-aminated SBA-15	199.2	2.4	0.38

[a]specific surface area, calculate from multi-point BET analysis.
[b]The pore dimeter calculated from the adsorption part of the isotherm using the BJH method.
[c]Total pore volume calculated from the BJH method.

Adsorption studies

- Impacts of pH

The experiments of PH optimization were conducted in the pH range of 2-12, beginning concentration of 40 ppm, adsorbent dosage of 0.02 g and 120 minutes contact time. As can be seen in the Fig. 6a and Fig. 6b, it was at the pH of 2 that the greatest removal do dye happened. At lower pH, the adsorbent surface and tannin take positive charge with the absorption of H^+. So, strong attraction of electrostatic happens between the negative charges of dyeing molecules and the positive charge of the surface of the adsorbent at pH of 2. Higher values of pH increase the negative charges and decrease the positive charges of the surface. So, it enhances the electrostatic repulsion of the tannin negative charges and the anionic dye molecules. Therefore, this phenomenon causes the decrease of adsorption capacity [26]. In other word, the competition between OH^- ions and anionic molecules of acid blue 62 in alkaline condition causes low adsorption capacity.

- Impact of adsorbent dosage

Fig. 7 illustrates the impact of adsorbent dosage. As can be seen, adsorbent dosage is proportional to dye removal efficiency up to the optimum value of dosage. Extra accumulation of adsorbent in dye solution reduces the acceptor sites and inhibits the adsorption process [27]. The optimum value of adsorbent dosage was found to be 0.03 g while the beginning concentration of the dye, PH, temperature and the contact time were kept at 40 ppm, 2, 25 °C and 120 minutes, respectively. The rest of experiments was performed by the optimum value of dosage.

- Impact of the contact time at various temperatures

In order to investigate the temperature effects and contact time on the acid blue 62 adsorption, experiments were performed at temperatures of 25, 35 and 45 °C at different time intervals from 0 to 120 minutes. Fig. 8 shows that for all temperatures, the process of adsorption takes place immediately for all temperatures in the first 15 minutes. As can be seen, adsorption would be completed after 90 minutes and the adsorption equilibrium would be obtained. Therefore, 90 minutes of contact time was chosen as the time of equilibrium and was applied for the remains of the experiments. The rise of contact time accelerates the accumulation of dye molecules over the adsorbent surface and

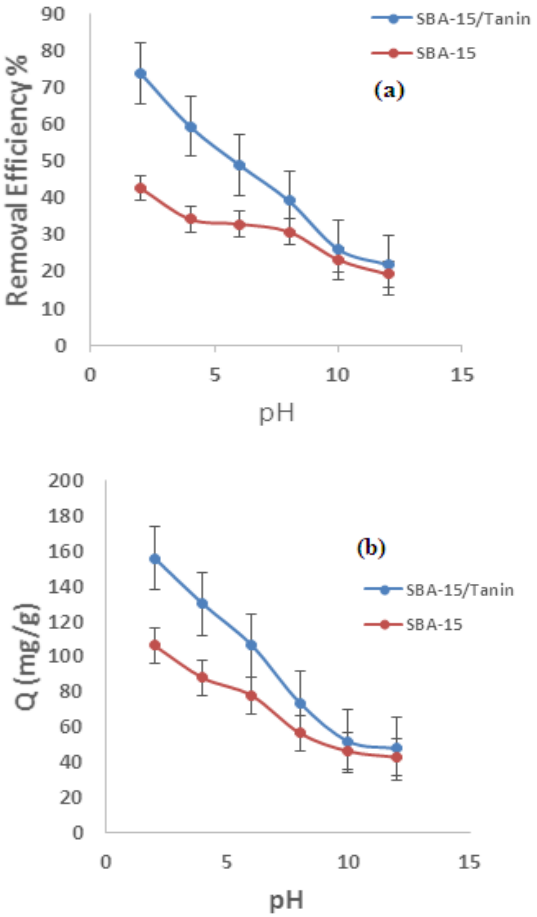

Fig. 6: Effect of adsorbent dosage on (a) removal efficiency and (b) dye adsorption amount of acid blue 62.

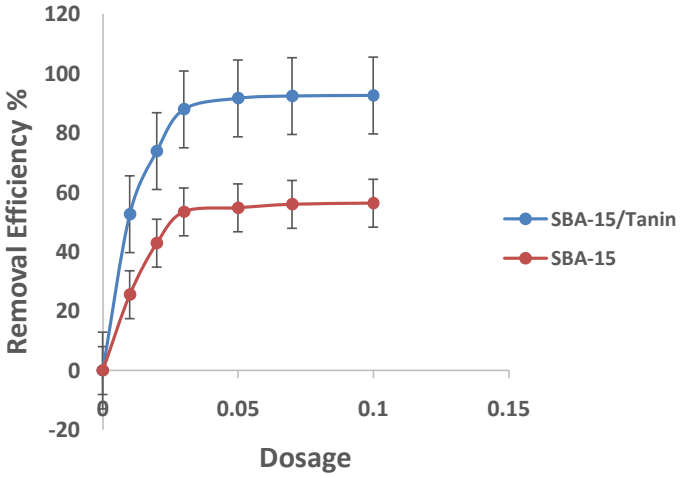

Fig. 7: Effect of contact time and temperature on adsorption capacity (initial dye concentration: 40 ppm, adsorbent dosage: 0.03 g, pH of 2).

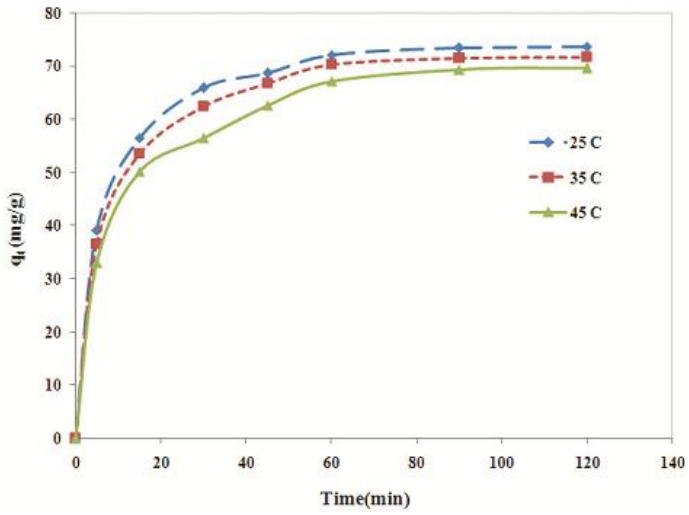

Fig. 8: Effect of temperatures in the range of 25 to 45°C on thermodynamic parameters (initial dye concentration: 40 ppm, adsorbent dosage: 0.03 g, pH of 2, and contact time of 90 min).

prevents dye molecules from being deeply diffused into the sites with higher energy. The single and flat adsorption curves show that the adsorbate gives monolayer coverage to the adsorbent surface [28]. Besides, ascending temperature (up to 45 °C) limits the adsorption capacity. Therefore, adsorption process is exothermic. The nature of the adsorption process can be the best reason for this phenomenon.

Adsorption kinetics

Kinetic models of adsorption process can determine the controlling steps of the adsorption rate containing either mass transfer or chemical reaction. In order to decide which kinetic model is superior, four significant kinetic models including intra-particle diffusion model, pseudo-second order, pseudo-first order, and Elovich models were applied.

- Intra-particle diffusion model

Intra-particle diffusion model was presented by Weber and Morris [29] as following equation:

$$q_t = k_p t^{0.5} + C \quad (3)$$

Where *C* is the intercept of equation (3) signifying of the boundary layer effects (see Table

2) and k_p is defined as the diffusion rate constant of the intra-particle (mg g^{-1} $min^{-0.5}$) which can be determined from plotting of q_t (mg/g) versus $t^{0.5}$. As Fig. 9c shows, the linear graph does not pass from the main source. So there are other rate-controlling processes and boundary layer effects than the intra-particle diffusion which act as a controlling process of the adsorption kinetic. The investigations of other researchers prove the present proposed kinetic mechanism [1, 13, 30].

- The pseudo-first order kinetic model

Lagergren proposed the Pseudo first order kinetic model as a following relation [31]:

$$\ln(q_e - q) = \ln(q_e) - k_1 t \quad (4)$$

Where q_e (mg g^{-1}) and rate constant k_1 (min^{-1}) are determined from the plot of $\ln(q_e - q_t)$ versus *t* (Fig. 9a). The results are shown in Table 2.

- The pseudo-second order kinetic model

The following equation [31] can define the pseudo second order kinetic model:

$$t/q = 1/k2qe2 + t/qe \quad (5)$$

q_e and k_2 are calculated from the slope and intercept of the straight lines (t/q_t versus *t* (Fig. 9b), respectively (Table 2).

- The Elovich model

The equation of Elovich or Roginsky–Zeldovich can be basically described as follows [32]:

$$q = (1/\beta_E).\ln(\alpha_E.\beta_E) + (1/\beta_E).\ln t \quad (6)$$

The quantity of dye which is adsorbed at the given time of t (mg/g) is q_t and α is considered as a constant which is related to chemisorption rate, and another constant that shows the degree of surface coverage is β. The intercept and slope of the plot of q_t versus lnt can be used to measure the two constants of (α and β) (Fig. 9d).

Fig. 9d shows a plot of the Elovich equation. In this case, a relationship which was linear was seen between adsorbed dye, q_t, and ln t throughout the sorption period, which had the correlation coefficient of 0.969 (Table 2). Table 2 depicts all the kinetic constants calculated from the Elovich equation and three other kinetic models. As the data shows, the values of α and β have shown appropriate for highly heterogeneous systems of which the adsorption of acid blue 62 onto adsorbent is almost such a case, although the Elovich equation does not give any mechanistic evidence. The results of Table 2 demonstrate a great degree of correlation which exists between the experimental data and the theoretical data prognosticated by pseudo-second order model. The estimated value of q_e from pseudo-second order model is seen to be close to the experimental value ($q_{e,exp}$ = 73.34 mg/g). So, the first order model cannot show the adsorption kinetic as well as the pseudo-second kinetic model. Other researchers have published almost similar results for removing of Congo red by 3-aminopropyl-triethoxysilane functionalized SBA-15 (APTES/SBA-15) [30], the removal of Acid Blue 113 by penta ethylene hexamine functionalized SBA-3 (SBA-3/PEHA) [33] and adsorption of acid red 18 (AR18) by natural polymer chitosan (CTS / SBA-15) [14] .

CONCLUSION

In the present study, hexagonal mesoporous silicate (SBA-15) modified by tannin, was synthesized and then was applied as a new composite adsorbent (Tannin-Animated SBA-15) for acid blue 62 removal. The results indicated that the Tannin-Animated SBA-15 enjoys high capacity of adsorption (1000 mg/g) and of quick adsorption kinetic of dye removal. Effective distribution of tannin on the surface and in the pores of nano-composite was proved by decline of special surface area (from the BET equation), the volume and the average pore size (from the BJH method) of SBA-15. Hence, Tannin-Animated SBA-15 could be stated as the useful absorbent for removing the pollutant.

Kinetic investigations showed that there is a proper compatibility between the pseudo-second-order kinetic model and the experimental data. Study on the intra-particle diffusion model also

Table 2: Parameters of various kinetic models adsorption of acid blue 62 on tannic acid-aminated SBA at 298K.

Elovich			Pseudo-first order			Pseudo-second order			Intraparticle model			
α_E (mg/g.min)	β_E (g/mg)	R^2	k_1 (1/min)	$q_{e,cal.}$ (mg/g)	R^2	k_2 (g/mg.min)	$q_{e,cal}$ (mg/g)	R^2	C (mg/g)	K_p (mg/g.$min^{0.5}$)	R^2	$q_{e,exp.}$ (mg/g)
73.576	0.083	0.969	0.057	39.800	0.991	0.002	83.330	0.999	4.556	35.620	0.857	73.340

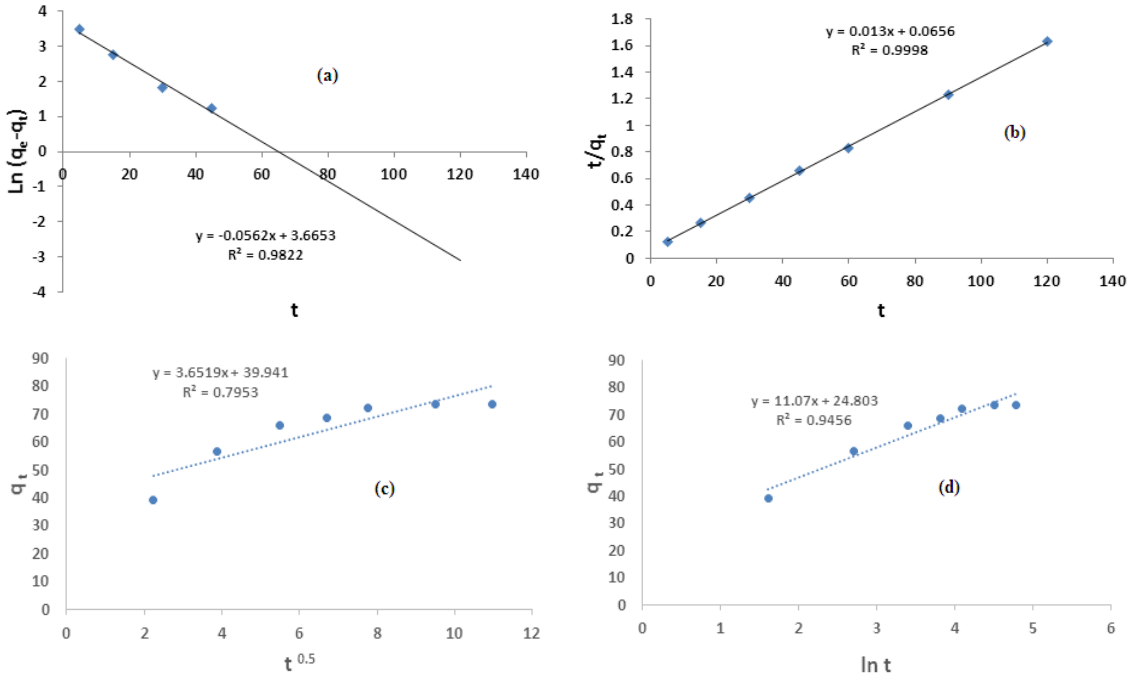

Fig. 9: (a) pseudo-first order, (b) pseudo-second order, (c) Intra-particle diffusion and (d) Elovich kinetic models for adsorption of acid blue 62 onto SBA-15/Tannin at 298K.

demonstrated that boundary layer and intra-particle diffusion have significant effect on the kinetic of adsorption process.

CONFLICT OF INTEREST

The authors declare that there is no conflict of interests regarding the publication of this manuscript.

REFERENCES

[1] Binaeian E., Seghatoleslami N., Chaichi M. J., (2016), Synthesis of oak gall tannin-immobilized hexagonal mesoporous silicate (OGT-HMS) as a new super adsorbent for the removal of anionic dye from aqueous solution. *Desalin. Water. Treat*. 57: 8420–8436.

[2] Aksu Z., Isoglu I. A., (2006), Use of agricultural waste sugar beet pulp for the removal of Gemazol turquoise blue-G reactive dye from aqueous solution. *J. Hazard. Mater*. B137: 418–430.

[3] Baek M. H., Ijagbemi C. O., Kim D. S., (2010), Removal of malachite green from aqueous solution using degreased coffee bean. *J. Hazard. Mater*. 176: 820–828.

[4] Hameed B. H., Ahmad A. A., (2009), Batch adsorption of methylene blue from aqueous solution by garlic peel, an agricultural waste biomass. *J. Hazard. Mater*. 164: 870–875.

[5] Hameed B. H., El-Khaiary M. I., (2008), Removal of basic dye from aqueous medium using a novel agricultural waste material: Pumpkin seed hull. *J. Hazard. Mater.* 155: 601–609.

[6] Akar T., Tosun I., Kaynak Z., Ozkara E., Yeni O., Sahin E. N., Akar S. T., (2009), An attractive agro-industrial by- product in environmental cleanup: Dye biosorption potential of untreated olive pomace. *J. Hazard. Mater.* 166: 1217–1225.

[7] Khaled A., El-Nemr A., El-Sikaily A., Abdelwahab O., (2009), Removal of direct N Blue-106 from artificial textile dye effluent using activated carbon from orange peel: Adsorption isotherm and kinetic studies. *J. Hazard. Mater*. 165: 100–110.

[8] Gupta N., Kushwaha A. K., Chattopadhyaya M. C., (2011), Application of potato (Solanum tuberosum) plant wastes for the removal of methylene blue and malachite green dye from solution. *Arab. J. Chem*. 9: S707-716.

[9] Tunc O., Tanacı H., Aksu Z., (2009), Potential use of cotton plant wastes for the removal of Remazol Black B reactive dye. *J. Hazard. Mater*. 163: 187–198.

[10] Ozacar M., Sengil I. A., Turkmenler H., (2008), Equilibrium and kinetic data and adsorption mechanism for adsorption of lead onto valonia tannin resin. *Chem. Eng. J.* 143: 32–42.

[11] Bagda E., (2012), The feasibility of using Rosa canina galls as an effective new biosorbent for removal of methylene blue and crystal violet. *Desalin. Water. Treat*. 43: 63-75.

[12] Yurtsever M., Sengil I. A., (2009), Biosorption of Pb (II) ions by modified quebracho tannin resin. *J. Hazard. Mater.* 163: 58–64.

[13] Shafiabadi M., Dasht A., Tayebi H. A., (2016), Removal of Hg (II) from aqueous solution using polypyrrole/SBA-15 nanocomposite: Experimental and modeling. *Synth. Metal.* 212: 154–160.

[14] Gao Q., Zhu H., Luo W. J. , Wang S., Zhou C. G., (2014), Preparation, characterization, and adsorption evaluation of chitosan-functionalized mesoporous composites. *Microporous. Mesoporous. Mater.* 193: 15–26.

[15] Asouhidou D., Triantafyllidis K. S., Lazaridis N. K., Matis K. A., (2009), Adsorption of remazol Red 3BS from aqueous solutions using APTES- and cyclodextrin-modified HMS-type mesoporous silicas. *Colloids Surf. A.* 346: 83–90.

[16] Torabinejad A., Nasirizadeh N., Yazdanshenas M. E., Tayebi H. A., (2016), Synthesize and characterization of Aminosilane functionalized MCM-41 for removal of anionic dye: Kinetic and thermodynamic study. *Int. J. Nano. Dimens*. 7: 295-307.

[17] Huang X., Liao X., Shi B., (2010), Tannin-immobilized mesoporous silica bead (BT–SiO_2) as an effective adsorbent of Cr (III) in aqueous solutions. *J. Hazard. Mater.* 173: 33–39.

[18] Zhao D., Huo Q., Feng J., Chmelka B. F., Stucky G. D., (1998), Nonionic triblock and star diblock copolymer and oligomeric surfactant syntheses of highly ordered, hydrothermally stable, mesoporous silica structures*. J. Am. Chem. Soc.* 120: 6024–6036.

[19] Huang X., Wang Y., Liao X., Shi B., (2010), Adsorptive recovery of Au^{3+} from aqueous solutions using bayberry tannin-immobilized mesoporous silica. *J. Hazard. Mater.* 183: 793–798.

[20] Falcao L., Eduarda M., Araujo M., (2013), Tannins characterization in historic leathers by complementary analytical techniques ATR-FTIR, UV-Vis and chemical tests. *J. Cultural. Heritage*. 14: 499-508.

[21] Grishechko L. I., Amaral-Labat G., Szczurek A., Fierro V., Kuznetsov B. N., Pizzi A., Celzard A., (2013), New tannin–lignin aerogels. *Ind. Crops Prod*. 41: 347– 355.

[22] Bulut M. C. E., Ornek A., Ozacar M., (2013), Synthesis and characterization of valonea tannin resin and its interaction with palladium (II), rhodium (III) chloro complexes. *Chem. Eng. J.* 221: 146–158.

[23] Gurung M., Adhikari B. B., Kawakita H., Ohto K., Inoue K., Alam S., (2011), Recovery of Au(III) by using low cost adsorbent prepared from persimmon tannin Extract. *Chem. Eng. J.* 174: 556– 563.

[24] Yurtsever M., Sengil I. A., (2012), Adsorption and desorption behavior of silver ions onto valonia tannin resin. *Trans. Nonferrous Met. Soc. China.* 22: 2846-2854.

[25] Liu J., Ma S., Zang L., (2013), Preparation and characterization of ammonium-functionalized silica nanoparticle as a new adsorbent to remove methyl orange from aqueous solution. *Appl. Surf. Sci.* 265: 393– 398.

[26] Tayebi H. A., Dalirandeh Z., Shokuhi Rad A., Mirabi A. Binaeian E., (2016), Synthesis of polyaniline/Fe3O4 magnetic nanoparticles for removal of reactive red 198 from textile waste water: kinetic, isotherm, and thermodynamic studies. *Desalin. Water. Treat*. 57: 22551-22563.

[27] Shabandokht M., Binaeian E., Tayebi H. A., (2016), Adsorption of food dye Acid red 18 onto polyaniline-modified rice husk composite: isotherm and kinetic analysis. *Desalin. Water. Treat.* 57: 27638-27650.

[28] Zhong Q., Yue Q. Y., Li Q., Xu X., Gao B. Y., (2011), Preparation, characterization of modified wheat residue and its utilization for the anionic dye removal. *Desalination*. 267: 193–200.

[29] Jr W. J., Weber J. C. M., (1963), Kinetics of adsorption on carbon from solution. *J. Sanit. Eng. Div. Am. Soc. Civ. Eng.* 89: 31–60.

[30] Laaz I., Stébéa M., Benhamou A., Zoubir D., Blin J., (2016), Influence of porosity and surface modification on the adsorption of both cationic and anionic dyes. *Colloids Surf. A: Physicochem. Eng. Aspects.* 490: 30–40.

[31] Li W., Tang Y. , Zeng Y., Tong Z., Liang D., Cui W., (2012), Adsorption behavior of Cr (VI) ions on tannin-immobilized activated clay. *Chem. Eng. J.* 193: 88–95.

[32] Inyinbor A. A., Adekola F. A., Olatunji G. A., (2016), Kinetics, isotherms and thermodynamic modeling of liquid phase adsorption of Rhodamine B dye onto Raphia hookerie fruit epicarp. *Water. Resour. Ind*. 15: 14-27.

[33] Anbia M., Salehi S., (2012), Removal of acid dyes from aqueous media by adsorption onto amino-functionalized nanoporous silica SBA-3. *Dyes. Pigments*. 94: 1-9.